Improving Maraviroc Oral Bioavailability by Formation of Solid Drug Nanoparticles

Alison C. Savage,[a*] Lee M. Tatham,[b*] Marco Siccardi,[b] Trevor Scott,[c] Manoli Vourvahis,[d] Andrew Clark,[e] Steve P. Rannard,[a#] Andrew Owen.[b#]

a. Department of Chemistry, University of Liverpool, Crown Street, Liverpool. L69 7ZD, UK
b. Department of Molecular and Clinical Pharmacology, University of Liverpool, 70 Pembroke Place, Liverpool. L69 3GF, UK
c. ViiV Healthcare, Five Moore Drive, Research Triangle Park, North Carolina, USA.
d. Pfizer, 235 East 42nd Street, New York, New York, USA.
e. ViiV Healthcare UK Limited, 980 Great West Road, Brentford, Middlesex, TW8 9GS, UK

*Both authors contributed equally to the work

#Authors for correspondence

Abstract

Oral drug administration remains the preferred approach for treatment of HIV in most patients. Maraviroc (MVC) is the first in class co-receptor antagonist, which blocks HIV entry into host cells. MVC has an oral bioavailability of approximately 33%, which is limited by poor permeability as well as affinity for CYP3A and several drug transporters. While once-daily doses are now the favoured option for HIV therapy, dose-limiting postural hypotension has been of theoretical concern when administering doses high enough to achieve this for MVC (particularly during coadministration of enzyme inhibitors). To overcome low bioavailability and modify the pharmacokinetic profile, a series of 70 wt% MVC solid drug nanoparticle (SDN) formulations (containing 30wt% of various polymer/surfactant excipients) were generated using emulsion templated freeze-drying. The lead formulation contained PVA and AOT excipients ($^{MVC}SDN_{PVA/AOT}$), and was demonstrated to be fully water-dispersible to release drug nanoparticles with z-average diameter of 728 nm and polydispersity index of 0.3. *In vitro* and *in vivo* studies of $^{MVC}SDN_{PVA/AOT}$ showed increased apparent permeability of MVC, compared to a conventional MVC preparation, with *in vivo* studies in rats showing a 2.5-fold increase in AUC (145.33 vs. 58.71 ng.h ml^{-1}). MVC tissue distribution was similar or slightly increased in tissues examined compared to the conventional MVC preparation, with the exception of the liver, spleen and kidneys, which showed statistically significant increases in MVC for $^{MVC}SDN_{PVA/AOT}$. These data support a novel oral format with the potential for dose reduction while maintaining therapeutic MVC exposure and potentially enabling a once-daily fixed dose combination product.

Keywords

Maraviroc; Freeze drying; Bioavailability; Nanodispersion; Nanomedicine; Pharmacokinetics

Introduction

Oral administration of antiretroviral therapy (ART) has been the standard approach in reducing patient mortality [1], and usually involves co-administration of three drugs from at least two different classes [2]. Maraviroc (MVC) is an entry inhibitor which targets the CCR5 co-receptor to prevent entry of CCR5-tropic virus into T-cells [3]. Oral dosing presents a simple route for self-administration but is often limited by low bioavailability. MVC is a class III molecule according to the Biophysical Classification System (aqueous solubility = 0.0106 mg/mL, logP = 4.37, pKa = 7.3) and a substrate for cytochrome P450 3A (CYP3A) and drug transporters, which contribute to its low bioavailability in humans, and up to 60% is estimated to be metabolised at first pass [1, 4-8]. In humans, the oral bioavailability of MVC is estimated to be approximately 33% for a 300 mg dose, with absolute oral bioavailability of 23.1% at 100 mg [9].

The World Health Organisation (WHO) estimate that over 36 million people were living with HIV globally in 2016, with only 19.5 million receiving access to ART. The most affected region is Africa which, according to WHO, accounts for approximately two thirds of global new HIV infections and 25.6 million people living with HIV. Global efforts are being made to improve access to ART, with WHO aiming to increase the number of patients receiving ART from approximately 50% to 90% by 2020 [2]. One way in which access to antiretroviral drugs can be increased is by reduction in the doses required for viral suppression, which in turn would reduce the manufacturing cost of the therapies and improve availability for charitable access in less economically developed countries.

Many drugs may be currently given at higher doses than necessary, which has resulted in several recent studies to assess the efficacy of reduced-doses of conventional formulations [10-13]. However, nanomedicine approaches offer further opportunities for dose reduction while maintaining plasma pharmacokinetic exposure. Indeed, recently we reported an emulsion-templated freeze drying (ETFD) approach to prepare solid drug nanoparticles (SDNs) for the antiretroviral drugs efavirenz and lopinavir, which resulted in much higher plasma concentrations relative to conventional preclinical formulations following oral administration [14-16].

MVC-containing ART regimens require twice-daily administration to patients to maintain plasma concentrations within the therapeutic range over the dosing interval. Current dosing recommendations for a MVC 300 mg twice-daily dose in adults and adolescents is aimed at targeting a median C_{avg} of 131 ng ml^{-1}, an established parameter relating the MVC efficacy, a C_{max} of 724.9 ng ml^{-1} and C_{min} between 25 and 50 ng ml^{-1} depending on the regimen followed [3, 17, 18]. Preferred ART regimens currently involve once-daily dosing, but MVC dose has not been increased to achieve this due to the theoretical risk of dose-limiting postural

hypotension, which was seen in clinical development and related predominantly to MVC maximum plasma concentrations (C_{max}) [19]. MVC efficacy has been associated with average plasma concentrations (C_{avg}) in several studies [16]. Therefore, the aim of this study was to develop a MVC SDN formulation with higher bioavailability and lower C_{max}:C_{avg} ratio to support dose reduction and once-daily dosing, respectively. Perhaps more importantly, a lower dose formulation of MVC may also better support development of MVC-containing fixed dose combination (FDC) products.

The current study reports the development of MVC SDNs generated using ETFD. Polymer and surfactant excipients were first studied using a small scale high-throughput screening approach to select the most suitable excipients for reproducible scale-up and manufacture. Subsequently, SDN lead selection was conducted by screening apparent permeability (P_{app}) across Caco-2 monolayers, before confirmation of improved pharmacokinetic performance after oral administration to rats.

Experimental

Materials were purchased and used as received without further purification: α-tocopherol poly(ethylene glycol) succinate (TPGS), poly(ethyleneoxide)$_{20}$ sorbitan monolaurate (Tween 20), poly(ethyleneoxide)$_{20}$ sorbitan monooleate (Tween 80), sodium deoxycholate (NDC), benzethonium chloride (hyamine), polyvinyl alcohol (PVA), hydroxymethyl propyl cellulose (HPMC), poly(ethylene oxide)101-block-poly(propylene oxide)56-block-poly(ethylene oxide)101 (Pluronic F127), poly(ethylene oxide)$_{80}$-block-poly(propylene oxide)$_{27}$-block-poly(ethylene oxide)$_{80}$ (Pluronic F68), sodium 1,4-bis(2-ethylhexoxy)-1,4-dioxobutane-2-sulfonate (AOT), Dimethyl sulfoxide (DMSO), acetonitrile, 30% hydrogen peroxide, glacial acetic acid, (4-(2-hydroxyethyl)-1-piperazineethanesulfonic acid (HEPES), bovine serum albumin (BSA), phosphate buffered saline (PBS), Hanks' balanced salt solution (HBSS) and trypsin-EDTA (Sigma–Aldrich, Dorset, UK); poly(ethylene glycol)$_{15}$-hydroxystearate (Solutol) and poly(vinyl alcohol)-graft-poly(ethylene glycol) copolymer (Kollicoat® Protect) (BASF, Royal Tunbridge Wells, UK); poly(ethylene glycol) (PEG 1000) and poly(vinylpyrrolidone) (PVP K30) (Fluka Chemicals, Dorset, UK); chloroform (Fisher Scientific, Loughbrough, UK); MVC was kindly donated by ViiV healthcare (UK) and ^{3}H MVC was purchased from Moravek (California, USA). All other chemicals and reagents were purchased from Sigma-Aldrich (UK) and used as received, unless stated otherwise. Soluene-350 was purchased from PerkinElmer (US). Ultima Gold liquid scintillation fluid was purchased from Meridian biotechnologies (UK) and [^{14}C]-mannitol was purchased from American Radiolabelled Chemicals (US). Transwell permeable supports with a 0.4 µm pore size were purchased from Corning (US). Caco-2 cells were purchased from American Type Culture Collection (ATCC, US).

Emulsion-templated freeze drying of maraviroc SDNs

Aqueous stock solutions of polymer and surfactants were prepared at 22.5 mg ml^{-1}, MVC was prepared was at 70 mg ml^{-1} in dichloromethane. An example 70 wt% drug loaded SDN was prepared as followed: Solutions were prepared at a 4:1 water:oil ratio, with 90 µl polymer, 45 µl surfactant and 265 µl water added to 100 µl MVC in dichloromethane (DCM). The resulting mixture was emulsified with a Covaris S2x for 30 seconds with a duty cycle of 20, intensity of 10 and 500 cycles/burst in frequency sweeping mode, after which samples were immediately cryogenically frozen. The initial screening consisted of a 49-sample library which was prepared as above and lyophilised using a Virtis benchtop K freeze dryer for 48 hours. Samples were immediately sealed until analysis.

Physical characterisation of MVC SDN library

Immediately prior to analysis, samples were dispersed in a volume of water to give 1 mg/ml with respect to drug concentration. The z-average diameter (nm) of the SDNs was measured using dynamic light scattering (DLS; Malvern Zetasizer Nano ZS) using automatic measurement optimisation. Zeta potential was also measure with the Malvern Zetasizer Nano ZS, using the Smoluchowski model; both DLS and Zeta potential measurements used Malvern Zetasizer software version 7.11 for data analysis. Powder X-ray diffraction (XRD) measurements were collected in transmission mode on the solid monolith samples held on a thin Mylar film in aluminum well plates on a Panalytical X'Pert PRO MPD instrument with X'Pert Operator Interface (version 1.0b) software.

Cell culture and maintenance

Caco-2 cells were maintained in Dulbecco's Modified Eagle's Medium (DMEM) supplemented with 15% fetal bovine serum (FBS) (Gibco, UK). Cells were incubated at 37ºC, 5% CO_2. Caco-2 cells were sub-cultured once ~85% confluent. Cell counting and viability assessments were determined using propidium iodide exclusion on a NucleoCounter (Denmark).

Transcellular permeability of maraviroc across Caco-2 monolayers

Transwells were seeded with 1.5 x 10^5 cells per well and propagated to a monolayer over 21-days. During propagation, the media was aspirated from both apical and basolateral compartments and replaced with an equal volume of fresh pre-warmed (37ºC) media every other day, yielding transepithelial electrical resistance (TEER) values of >1000 Ω. After 21-days, the media was aspirated, wells washed with pre-warmed (37ºC) HBSS and replaced with either DMSO dissolved MVC (<0.5% DMSO) or MVC nanodispersions, spiked into transport buffer, to a final concentration of 10 µM MVC with a specific activity of 25 µCi/mg [^{3}H]-MVC. The suspensions were added to either apical or basolateral compartments and transport buffer added to the opposing chamber to quantify transport in both apical-to-basolateral (A>B) and basolateral-to-apical (B>A) directions. One-hundred microliters was sampled hourly from the opposing acceptor chamber over 4 h and replaced with an equal volume of fresh pre-warmed (37ºC) transport buffer. Collected samples were placed into empty 5 ml scintillation vials before mixing with liquid scintillation fluid (4 ml). Radioactivity was determined as disintegrations per minute (DPM) using a Packard Tri-carb 3100TR liquid scintillation counter. Apparent permeability (P_{app}) was determined by the amount of MVC transported over time using equation (1).

$$P\text{app} = \frac{(\mathrm{d}Q/\mathrm{d}t) \times v}{A \times C_0}$$

(1)

Where (d*Q*/d*t*) is the amount per time; *v* is the volume of the receiver compartment; *A* is the surface area of the filter; and C_0 is the starting concentration of the donor chamber. Apparent oral absorption was calculated using the P_{app} values: (A>B)/(B>A).

To assess the integrity of the monolayer following the 4 h incubation, transport buffer was aspirated and the wells washed twice with pre-warmed (37ºC) HBSS. Subsequently, 0.1 ml of transport buffer containing [^{14}C]-mannitol (50 µM, 2 µCi/ml) was added to the apical compartment of the test and control wells and 0.55 ml of transport buffer was added to the basolateral compartments. The plates were incubated at 37ºC, 5% CO_2 for 1 h. Following incubation, 0.1 ml of the basolateral contents were sampled and placed into empty 5 ml scintillation vials before mixing with liquid scintillation fluid (4 ml). Radioactivity was determined as described above.

In vivo analysis of lead maraviroc nanodispersion

All animal work was conducted in accordance with the Animals (Scientific Procedures) Act 1986 (ASPA) implemented by the UK Home Office. The rodents were housed with environmental enrichment and a 12 h light/dark cycle at 21ºC ±2ºC. Free access to food and water was provided at all times. Following 7-days acclimatisation, adult male Wistar rats (280-330 g) (Charles River, UK) were dosed with 10 mg Kg^{-1} MVC at 10 µCi/mg, either as a conventional [^{3}H]-MVC preparation (<5% DMSO) or as a [^{3}H]-$^{MVC}SDN_{PVA/AOT}$ nanodispersion (lead MVC SDN formulation containing PVA and AOT as excipients), using a 7-cm curved gavage needle, four rats per condition. Subsequently, blood samples were collected (0.3 ml) at 0.5, 1.0, 1.5, 2.0 and 3.0 h post-dosing from the tail vein. At 4.0 h, the rats were sacrificed using cardiac puncture under terminal anaesthesia (isoflurane/oxygen), followed by immediate exsanguination of blood from the heart. Subsequently, an overdose of sodium pentobarbitone (Animalcare, UK) was administered using the same in situ puncture needle. Terminal tissue samples were collected, rinsed in PBS and dried on tissue before storing at -20ºC. Blood samples were collected in heparinised Eppendorf tubes and centrifuged at 3,000 rpm for 5 min. The plasma layer was collected and stored at -20ºC prior to analysis.

Quantification of radiolabelled plasma and tissues

Plasma samples (0.1 ml) were transferred to scintillation vials before adding scintillation fluid (4 ml) (Meridian Biotechnologies, UK) and scintillation counting using a Packard Tri-carb 3100TR. Each dissected tissue was weighed individually and approximately 100 mg was placed into 20 ml scintillation vials. Tissue samples were submerged in 1 ml Soluene-350 (PerkinElmer, US) and incubated in a water bath at 50^{o}C for 18 h. After allowing to cool to room temperature, 0.2 ml of a 30% hydrogen peroxide solution was added to the dissolved sample and incubated for 60 min at room temperature. Subsequently, 0.09 ml of glacial acetic acid was added to each sample and incubated for a further 15 min at 50^{o}C. Scintillation fluid (12 ml) was added to each sample and mixed via inversion. Scintillation counting was carried out using a Packard Tri-carb 3100TR.

Statistical analysis

Statistical analysis was performed using GraphPad Prism v.7 (US). Where statistical analysis is described, data normality was assessed with the Shapiro-Wilk test using StatsDirect v.3 (UK). Data were found to be normally distributed and unpaired, two-tailed t-tests were applied. Differences were considered statistically significant at *, $P<0.05$. Results are expressed as means and associated standard deviations. The pharmacokinetic parameters; maximum concentration (C_{max}), the time to C_{max} (T_{max}), trough concentrations (C_{min}) and the average concentration (C_{avg}) were derived from the concentration-time profiles. The area under the curve, (AUC_{0-4}) and half-life (t½) were calculated using PKSolver [20].

Results and discussion

Excipient determination by screen

As described above, MVC SDN library preparation was evaluated against a series of 49 binary polymer and surfactant excipients (seven polymers and seven surfactants) selected from the U.S. Food and Drug Administration Center for Drug Evaluation and Research list of Inactive Ingredients [21]. MVC was dissolved in DCM, and added to an aqueous mixed solution of polymer and surfactant to generate a 4:1 ratio of water:oil. This ratio was chosen due to its proven success in producing SDNs using the ETFD strategy [15]. The samples were sonicated and immediately cryogenically frozen to preserve the emulsion template before freeze drying. The rapid cooling generates a thermal shock to the dispersed and continuous phases of the emulsion, forcing the phases into a super-saturated regime and generating solid solvent regions; where the effective removal of solvent (water or DCM) through crystallisation occurs within an amorphous region, this also increases the concentration of the solute in the amorphous zones enabling subsequent precipitation or crystallisation of the MVC to occur.

The resulting solid monoliths prepared by ETFD methods were dispersed in water and the nanodispersions of MVC were characterised using DLS to determine the z-average diameter and polydispersity of the dispersed sample. Samples were evaluated against previously-established critical criteria to progress to optimisation. Namely, all SDN candidates fully dispersed with no residual material, had a z-average diameter <1000 nm, standard deviation between each data set <15% and a polydispersity index <0.5. Initially the drug loading relative to polymer and surfactant excipient stabilisers was selected as 30 wt%. By applying this screening methodology, 9 polymer/surfactant combinations were identified meeting the criteria for candidate SDN formulations and subsequent optimisation studies (Fig. 1A).

Optimisation of drug loading

The initial nine polymer and surfactant combinations found to be successful at 30 wt% were adjusted to incorporate higher MVC loadings; this process was deemed to be highly important as it establishes the potential for later scale-ability and viable commercial manufacture. In each case, the polymer/surfactant combinations were subjected to serial modifications to incorporate higher MVC loadings (targeting 70 wt% MVC) at the expense of the stabiliser excipient combinations. In general, adjusting the MVC-loading from 40-70 wt% created a change in the observed SDN diameter (measured by DLS) (table 1), with no particular trend observed; a loose positive correlation between diameter and MVC loading was seen but this trend was not clearly established across all SDN candidates, with some maintaining similar sizes at all MVC loadings (Fig. 1B). The highest obtainable MVC loading achieved, and hence

the lowest corresponding polymer and surfactant content, was 70 wt% and three different formulations achieved this reproducibly. As seen in previous ETFD studies [14, 15, 22], such high drug content is a clear benefit of the ETFD strategy as techniques such as nano-milling and high-pressure homogenisation rarely reach drug contents above 30 wt% in their dried and re-dispersible form [23].

The three solid 70 wt% MVC-loaded SDN formulations which exhibited greatest reproducibility all contained the polymer PVA, which has also been found previously to be a successful polymer for producing stable SDN candidates from other antiretroviral drugs [14, 15]. The surfactants used in the successful SDNs of MVC were tween 80, NDC and AOT. The three formulations fully dispersed in water to give particles with diameters spanning 650-850 nm (table 2). $^{MVC}SDN_{PVA/AOT}$ exhibited a broader distribution than the other two formulations, resulting in a slightly larger polydispersity index. However, because the monolith is known to fully disperse upon the addition of water, the particle size distribution was not considered a reason to exclude from later pharmacological studies. The zeta potential for the three formulations were all negative, with the $^{MVC}SDN_{PVA/TW80}$ and $^{MVC}SDN_{PVA/NDC}$ having zeta potentials closer to neutrality than $^{MVC}SDN_{PVA/AOT}$, presumably due to the nature of the negative charge associated with the AOT surfactant. Analysis of $^{MVC}SDN_{PVA/AOT}$ by XRD shows the process of emulsion-templated freeze drying renders the MVC amorphous (fig. S2). Studies of a sample stored at room temperature also indicates that the SDN formulation maintains its amorphous state even after 20 months of storage.

In vitro permeation studies

Transwell plates can be used to support Caco-2 monolayers as the cells polarise, differentiate and form tight junctions [8]. The polarised monolayer resembles the functional lining of the small intestine and therefore offers an *in vitro* model for absorption across the human gut. The apical surface of the cells represents the surface exposed inside the gut while the basolateral surface of the cells represents the surface corresponding to the blood. Although not fully representative of a materials *in vivo* behaviour, the model provides exploratory data for further development and is widely used to screen drugs for absorption potential [24, 25].

MVC has previously been shown to have limited apical to basolateral permeation across Caco-2 monolayers and is a substrate for P-glycoprotein (P-gp) which contributes to enhanced basolateral to apical permeation, indicative of transporter-limited absorption [26], usually indicative of low oral bioavailability. The three lead SDN formulations, namely $^{MVC}SDN_{PVA/TW80}$, $^{MVC}SDN_{PVA/NDC}$ and $^{MVC}SDN_{PVA/AOT}$, were prepared at 70 wt% MVC using tritium-labelled MVC ([^{3}H]-MVC) to enhance the quantitative evaluation of their pharmacological behaviour;

transcellular permeation of the aqueous SDN nanodispersions was evaluated for both apical to basolateral and basolateral to apical permeability and compared to a conventional [^{3}H]-MVC preparation (<0.5% aqueous DMSO). The results outlined in Fig. 2 indicate improved apparent oral absorption ((P_{app}(A>B)/P_{app}(B>A)) of two of the nanodispersed [^{3}H]-MVC formulations ($^{MVC}SDN_{PVA/TW80}$ and $^{MVC}SDN_{PVA/AOT}$) when compared to a conventional [^{3}H]-MVC preparation; >8% and >74% increase after 1 h incubation was observed, respectively. Interestingly, this appeared to be largely driven by enhanced apical to basolateral permeation rather than a reduction in basolateral to apical permeation (Fig. 2, B). The mechanisms that underpin these observations are not clearly understood; however, various processes have been described which may account for the observed improvement, including paracellular permeation of intact particles, endocytosis of intact particles or indirect mechanisms which enable enhanced permeation of the dissolved drug [27]. The paracellular mechanism is characterised by permeation of small hydrophilic compounds between adjacent cells [28], although some nanoparticles have been shown to reversibly open tight junctions, increasing paracellular permeability, to allow larger nanoparticles to permeate across the epithelium and deliver drug-loaded nanoparticles to the systemic circulation [29]. Endocytosis is an energy-dependant transcellular transport mechanism that allows for the internalisation of nanoparticles within cells and subsequent transport of intact nanoparticles across the epithelium using membrane-bound carriers such as endosomes [30, 31]. However, enhanced oral absorption may not rely on the permeation of intact nanoparticles and instead, the nanoparticle may enhance drug dissolution afforded through supersaturation and increase localised drug concentrations in the gut which may ultimately saturate molecular processes and improve drug absorption / oral bioavailability [27, 32]. Interestingly, no correlation in the nanosuspensions size (D_z), zeta potential (ζ) or polydispersity and [^{3}H]-MVC permeability were identified in the study (data not shown).

The integrity of the Caco-2 monolayers was investigated using the hydrophilic low permeability marker [^{14}C]-mannitol following incubation with the conventional and each [^{3}H]-MVC SDN candidate. The integrity of the monolayers was assessed post-incubation to determine any potential cumulative damage to the monolayer over the 4 h. Co-incubation of each MVC preparation and the mannitol marker was not undertaken due to potential interactions of the ethanol containing [^{14}C]-mannitol and the MVC nanodispersions. The results outlined in Fig. S3 highlight [^{14}C]-mannitol P_{app} values of less than 0.953 x 10^{-6} cm s^{-1} indicating the Caco-2 monolayers remained intact following exposure to each treatment [25].

Maraviroc *in vivo* bioavailability studies

A rat model was used to investigate the *in vivo* oral pharmacokinetics of [^{3}H]-MVC using the aqueous dispersion of the $^{MVC}SDN_{PVA/AOT}$ candidate and a conventional MVC preparation (<5% aqueous DMSO). Each treatment group was orally-dosed at 10 mg Kg^{-1} [^{3}H]-MVC and blood samples were collected over 4 h to assess the different pharmacokinetic profiles. The results in Fig. 3 A. and Table 3. show increased C_{max} (50.74 vs. 26.52 ng ml^{-1}), increased C_{min} (25.83 vs. 8.16 ng ml^{-1}), increased AUC (145.33 vs. 58.71 ng.h ml^{-1}), increased C_{avg} (38.38 vs. 15.17 ng ml^{-1}) an equivalent T_{max} (time to achieve C_{max} after dosing; 1.5 h), reduced C_{max}:C_{min} ratio (1.96 vs. 3.25), reduced C_{max}:C_{avg} ratio (1.32 vs. 1.75) and increased apparent half-life (t½) (3.32 vs. 1.57 h) for the $^{MVC}SDN_{PVA/AOT}$ dosed rats compared to the conventional solution in aqueous DMSO. The observed improvements in MVC pharmacokinetics could potentially offer a number of benefits over conventional therapy. The results presented here highlight an increase in AUC and C_{min} for $^{MVC}SDN_{PVA/AOT}$, supporting a dose reduction strategy which ensures circulatory MVC concentrations remain efficacious, with an associated lower cost of therapy. The reduction in dose also has clear advantages for development of palatable and efficacious FDCs. MVC is generally well tolerated but C_{max}-driven postural hypotension has been described [3, 33], and C_{avg} is an established parameter relating to efficacy [28]. The favourable C_{max}:C_{avg} ratio reported here may enable development of a once-daily format, which maintains therapeutic exposure while avoiding the risk of concentration-dependent toxicities.

Gut metabolism is not believed to contribute significantly to the limited oral bioavailability that is observed for MVC in rats. Previous oral dosing studies in rats have shown that only a low abundance of metabolites are detectable in the circulating blood and over 79% of the parent compound is excreted [3]. It has been suggested that the limited oral bioavailability observed for MVC in rats is largely driven by incomplete absorption, which is estimated at 20-30%. In the same study, improved MVC oral absorption was noted in dogs and it was suggested that this may be due to the larger aqueous pores present in the gastrointestinal tract, aiding MVCs absorption [26, 34]. It is plausible that the nanosuspension enhances MVCs absorption in the rat gut leading to the observed improved pharmacokinetic profile.

In contrast, a mass balance model based on a 300 mg oral dose of MVC in healthy male human volunteers indicated that over 80% of the MVC dose was effectively absorbed. The same model predicted that the first-pass extraction of MVC is over 60% [9]. It has been demonstrated that MVC is predominantly metabolised in the liver by CYP3A with no significant involvement of any other CYP450 enzymes [35]. Despite this, unchanged MVC was shown to be the major circulating component in plasma (40-42%) and the major excreted component (33%) in humans [3, 35]. Interspecies pharmacokinetic scaling is complex [36] and the described differences in MVC absorption make the inference of potential pharmacokinetic benefits in humans difficult. However, it should be noted that the rats dosed with the MVC

SDNs appeared to sustain MVC plasma concentrations for longer compared to the conventional MVC preparation with an increased C_{avg} and increased half-life (t½) (3.32 vs. 1.57 h). The mechanisms underpinning the improvements in the MVC pharmacokinetic profile are likely to be complex and multifactorial. One possible explanation for the improvements is enhanced MVC lymphatic transport, which would ultimately contribute to the systemic exposure and potentially limit first-pass metabolism.

Lymph tissues are major sanctuary sites for HIV and viral replication occurs in these tissues even when the virus is undetectable in circulating blood [37, 38]. Distribution studies using intravenously administered [^{14}C]-MVC in rats have shown accumulation of [^{14}C]-MVC in lymph nodes both 1 and 4 h post-dose regardless of the lymph node location. Additionally, MVC concentrations were shown to be up to seven-fold higher in the lymph nodes than in circulating blood [39]. The penetration on MVC into these pharmacologically relevant tissues is likely to be important for infection management. A variety of nanoparticle technologies have been described with demonstrated or highlighted potential for enhanced lymphatic transport [40-42]. Microfold cells (M-cells) are a component of the intestinal epithelium that bind, transport and deliver macromolecules to the underlying Peyer's patches which are an organised component of the gut-associated lymphoid tissue (GALT) [43]. Enhanced uptake of intact nanoparticles or dissolved drug into M-cells potentially allows for effective drug delivery to the lymphatics, avoiding first-pass metabolism, and ultimately entering the systemic circulation for enhanced drug exposure [44, 45]. Future studies are planned to assess the accumulation of antiretrovirals into the lymphatics following oral dosing, using the described nanoparticle technology, to ascertain the relevance of this mechanism in drug delivery.

In addition to the enhanced pharmacokinetics, higher permeation was identified in most of the dissected tissues (Fig. 3 B). In particular, statistically significant increases in [^{3}H]-MVC were identified in the liver, spleen and kidney with a 2.2 (375.01 vs. 167.84 ng g^{-1}; P=<0.001), 1.6 (282.68 vs. 167.36 ng g^{-1}; P=<0.001) and 1.8-fold (231.31 vs. 130.47 ng g^{-1}; P=0.0057) increase, respectively. All other dissected tissues, except the heart and testis, were also shown to have increased MVC concentrations, however these were not considered statistically significant. These data must be interpreted in the context that plasma concentration was also higher for the SDN. Therefore, a direct comparison was not possible and the differences in tissue penetration may be directly related to the difference in plasma exposure. This also warrants further study, since the reported approach most likely delivers dissolved molecules into the systemic circulation rather than intact nanoparticles.

Nanoformulations similar to that described here have also attracted recent interest as long-acting injectables, providing prolonged therapeutic exposure for a period of weeks to months

from a single intramuscular dose [46]. The lead formulation ($^{MVC}SDN_{PVA/AOT}$) has also been investigated for this route of administration and the data are described elsewhere in this issue of the journal [47].

Conclusions

The nanomedicine reported here has the potential to enable new MVC dosing formats with the potential for once-daily dosing, while reducing doses required for effective viral suppression and improving the potential to develop novel ART FDCs. Dose reduction of antiretroviral drugs is also considered key to optimising the cost of treatment and improving charitable access to therapies for low and middle-income countries. By improving the oral bioavailability, the absorption of MVC into systemic circulation was improved, offering a clear strategy for reducing the amount of drug required for therapy. *In vitro* and *in vivo* studies showed improved apparent permeability of the $^{MVC}SDN_{PVA/AOT}$ formulation compared with conventional MVC preparations. Studies of tissue distribution revealed significant increases of MVC concentration in the spleen, liver and kidney, with distributions into other tissue showing slight increases in MVC with the $^{MVC}SDN_{PVA/AOT}$ compared with unformulated MVC. These improvements in oral bioavailability show the successful use of the ETFD technology to very rapidly identify viable SDN candidates that demonstrate significant benefits to justify continued progress towards nanomedicine production. Further study is now required to evaluate the implications for drug-interactions with known CYP3A or transporter inhibitors, but it may be expected that the magnitude of interaction may be smaller due to the apparent change in T½. The most successful, high drug-loaded, water-dispersible SDNs identified within this study require further work to translate through to scale-able processes, such as spray drying, which are required to establish clinical candidates that have potential for human evaluation [14].

Funding: This work was supported by ViiV Healthcare

Competing financial interests: The authors are co-inventors on patents relating to the application of nanotechnology to HIV drug delivery. AO and SR are co-founders of the University of Liverpool start-up company Tandem Nano Ltd. AO, SR and MS have also received funding from Merck, Janssen, AstraZeneca and Pfizer. TS and AC are employees of ViiV Healthcare, a GlaxoSmithKline Company, and holds stock in GlaxoSmithKline. MV is an employee of Pfizer and holds Pfizer stock/stock options.

References

[1] A. Sosnik and R. Augustine, "Challenges in oral drug delivery of antiretrovirals and the innovative strategies to overcome them," *Advanced Drug Delivery Reviews,* vol. 103, no. Supplement C, pp. 105-120, 2016/08/01/ 2016.

[2] *World Health Organisation, www.who.int/en/*.

[3] S. Abel, D. J. Back, and M. Vourvahis, "Maraviroc: pharmacokinetics and drug interactions," *Antiviral Therapy,* vol. 14, no. 5, pp. 607-618, 2009 2009.

[4] R. D. MacArthur and R. M. Novak, "Maraviroc: The first of a new class of antiretroviral agents," *Clinical Infectious Diseases,* vol. 47, no. 2, pp. 236-241, Jul 15 2008.

[5] B. Weatherley and L. McFadyen, "Maraviroc modelling strategy: use of early phase 1 data to support a semi-mechanistic population pharmacokinetic model," *British Journal of Clinical Pharmacology,* vol. 68, no. 3, pp. 355-369, 2009.

[6] M. Siccardi *et al.*, "Maraviroc is a substrate for OATP1B1 in vitro and maraviroc plasma concentrations are influenced by SLCO1B1 521 T>C polymorphism," *Pharmacogenet Genomics,* vol. 20, no. 12, pp. 759-65, Dec 2010.

[7] C. J. Forbes *et al.*, "Non-aqueous silicone elastomer gels as a vaginal microbicide delivery system for the HIV-1 entry inhibitor maraviroc," (in eng), *J Control Release,* vol. 156, no. 2, pp. 161-9, Dec 2011.

[8] M. J. O'Neil, P. E. Heckelman, P. H. Dobbelaar, K. J. Roman, C. M. Kenny, and L. S. Karaffa, *The Merck index : an encyclopedia of chemicals, drugs, and biologicals*, Fifteenth edition. ed. 2006.

[9] S. Abel, D. Russell, L. A. Whitlock, C. E. Ridgway, A. N. Nedderman, and D. K. Walker, "Assessment of the absorption, metabolism and absolute bioavailability of maraviroc in healthy male subjects," (in eng), *Br J Clin Pharmacol,* vol. 65 Suppl 1, pp. 60-7, 2008.

[10] M. Lanzafame, E. Lattuada, F. Rigo, A. Ferrari, A. Hill, and S. Vento, "Efficacy of a reduced dose of darunavir/ritonavir in a cohort of antiretroviral-naive and -experienced HIV-infected patients: a medium-term follow-up," *J Antimicrob Chemother,* vol. 70, no. 2, pp. 627-30, Feb 2015.

[11] S. Seang *et al.*, "Darunavir/ritonavir monotherapy at a low dose (600/100 mg/day) in HIV-1-infected individuals with suppressed HIV viraemia," *J Antimicrob Chemother,* Dec 5 2017.

[12] E. S. Group *et al.*, "Efficacy and safety of efavirenz 400 mg daily versus 600 mg daily: 96-week data from the randomised, double-blind, placebo-controlled, non-inferiority ENCORE1 study," *Lancet Infect Dis,* vol. 15, no. 7, pp. 793-802, Jul 2015.

[13] E. S. Group, "Efficacy of 400 mg efavirenz versus standard 600 mg dose in HIV-infected, antiretroviral-naive adults (ENCORE1): a randomised, double-blind, placebo-controlled, non-inferiority trial," *Lancet,* vol. 383, no. 9927, pp. 1474-1482, Apr 26 2014.

[14] M. Giardiello *et al.*, "Accelerated oral nanomedicine discovery from miniaturized screening to clinical production exemplified by paediatric HIV nanotherapies," *Nature Communications,* vol. 7, Oct 2016, Art. no. 13184.

[15] T. O. McDonald *et al.*, "Antiretroviral Solid Drug Nanoparticles with Enhanced Oral Bioavailability: Production, Characterization, and In Vitro-In Vivo Correlation," *Advanced Healthcare Materials,* vol. 3, no. 3, pp. 400-411, Mar 2014.

[16] H. Zhang *et al.*, "Formation and enhanced biocidal activity of water-dispersable organic nanoparticles," *Nat Nano,* 10.1038/nnano.2008.188 vol. 3, no. 8, pp. 506-511, 08//print 2008.

[17] S. M. Woollard and G. D. Kanmogne, "Maraviroc: a review of its use in HIV infection and beyond," (in eng), *Drug Des Devel Ther,* vol. 9, pp. 5447-68, 2015.

[18] J. Sierra-Madero *et al.*, "Efficacy and safety of maraviroc versus efavirenz, both with zidovudine/lamivudine: 96-week results from the MERIT study," (in eng), *HIV Clin Trials,* vol. 11, no. 3, pp. 125-32, 2010 May-Jun 2010.

[19] B. Weatherley, M. Vourvahis, and L. McFadyen, "Modeling of maraviroc pharmacokinetics in the presence of atazanavir/ritonavir in healthy volunteers and HIV-

1-infected patients," *12th International Workshop on Clinical Pharmacology of HIV Therapy,* vol. Abstract P_05, 2011.
[20] Y. Zhang, M. Huo, J. Zhou, and S. Xie, "An add-in program for pharmacokinetic and pharmacodynamic data analysis in Microsoft Excel," ed, 2010.
[21] "CDER list of inactive ingredients database: https://www.accessdata.fda.gov/scripts/cder/iig/index.cfm," ed.
[22] R. P. Bakshi *et al.*, "Long-acting injectable atovaquone nanomedicines for malaria prophylaxis," *Nature Communications,* vol. 9, p. 315, 2018.
[23] J. U. Junghanns and R. H. Muller, "Nanocrystal technology, drug delivery and clinical applications.," *International Journal of Nanomedicine,* vol. 3, no. 3, pp. 295-309, 2008.
[24] F. L. Hatton *et al.*, "Hyperbranched polydendrons: a new nanomaterials platform with tuneable permeation through model gut epithelium," (in eng), *Chem Sci,* vol. 6, no. 1, pp. 326-334, Jan 2015.
[25] R. Elsby, D. D. Surry, V. N. Smith, and A. J. Gray, "Validation and application of Caco-2 assays for the in vitro evaluation of development candidate drugs as substrates or inhibitors of P-glycoprotein to support regulatory submissions,," *Xenobiotica,* vol. 38, pp. 1140-1164, 2008.
[26] D. K. Walker *et al.*, "Species Differences in the Disposition of the Ccr5 Antagonist , Uk-427 , 857 , a New Potential Treatment for Hiv Abstract," *Drug Metab Dispos.,* vol. 33, pp. 587–595, 2005.
[27] L. M. Tatham, S. P. Rannard, and A. Owen, "Nanoformulation strategies for the enhanced oral bioavailability of antiretroviral therapeutics," *Therapeutic Delivery,* vol. 6, no. 4, pp. 469-490, 2015/04/01 2015.
[28] M. A. Shahbazi and H. A. Santos, "Improving oral absorption via drug-loaded nanocarriers: absorption mechanisms, intestinal models and rational fabrication," *Curr. Drug Metab.,* vol. 14, pp. 28-56, 2013.
[29] N. Salamat-Miller and T. P. Johnston, "Current strategies used to enhance the paracellular transport of therapeutic polypeptides across the intestinal epithelium," *Int. J. Pharm.,* vol. 294, pp. 201-216, 2005.
[30] B. Yameen, W. Il Choi, C. Vilos, A. Swami, J. Shi, and O. C. Farokhzad, "Insight into nanoparticle cellular uptake and intracellular targeting," *J. Control. Release,* vol. 190, pp. 485-499, 2014.
[31] P. L. Tuma and A. L. Hubbard, "Transcytosis: crossing cellular barriers.," *Physiol. Rev.,* vol. 83, pp. 871-932, 2003.
[32] P. Nkansah *et al.*, "Development and evaluation of novel solid nanodispersion system for oral delivery of poorly water-soluble drugs," (in eng), *J Control Release,* vol. 169, no. 1-2, pp. 150-61, Jul 2013.
[33] S. Abel *et al.*, "Assessment of the pharmacokinetics, safety and tolerability of maraviroc, a novel CCR5 antagonist, in healthy volunteers," (in eng), *Br J Clin Pharmacol,* vol. 65 Suppl 1, pp. 5-18, 2008.
[34] Y. L. He *et al.*, "Species differences in size discrimination in the paracellular pathway reflected by oral bioavailability of poly(ethylene glycol) and D-peptides," (in eng), *J Pharm Sci,* vol. 87, no. 5, pp. 626-33, May 1998.
[35] R. Hyland, M. Dickins, C. Collins, H. Jones, and B. Jones, "Maraviroc: in vitro assessment of drug-drug interaction potential," (in eng), *Br J Clin Pharmacol,* vol. 66, no. 4, pp. 498-507, Oct 2008.
[36] J. H. Lin and A. Y. H. Lu, "Commemorative issue: Applications and limitations of interspecies scaling and in vitro extrapolation in pharmocokinetics," *http://www.dmd.org,* 2017.
[37] C. V. Fletcher *et al.*, "Persistent HIV-1 replication is associated with lower antiretroviral drug concentrations in lymphatic tissues," (in eng), *Proc Natl Acad Sci U S A,* vol. 111, no. 6, pp. 2307-12, Feb 2014.
[38] J. N. Blankson, D. Persaud, and R. F. Siliciano, "The challenge of viral reservoirs in HIV-1 infection," (in eng), *Annu Rev Med,* vol. 53, pp. 557-93, 2002.

[39] D. K. Walker, S. J. Bowers, R. J. Mitchell, M. J. Potchoiba, C. M. Schroeder, and H. F. Small, "Preclinical assessment of the distribution of maraviroc to potential human immunodeficiency virus (HIV) sanctuary sites in the central nervous system (CNS) and gut-associated lymphoid tissue (GALT)," (in eng), *Xenobiotica,* vol. 38, no. 10, pp. 1330-9, Oct 2008.

[40] M. R. Aji Alex, A. J. Chacko, S. Jose, and E. B. Souto, "Lopinavir loaded solid lipid nanoparticles (SLN) for intestinal lymphatic targeting," (in eng), *Eur J Pharm Sci,* vol. 42, no. 1-2, pp. 11-8, Jan 2011.

[41] S. Jain, J. M. Sharma, A. K. Jain, and R. R. Mahajan, "Surface-stabilized lopinavir nanoparticles enhance oral bioavailability without coadministration of ritonavir," (in eng), *Nanomedicine (Lond),* vol. 8, no. 10, pp. 1639-55, Oct 2013.

[42] J. P. Freeling, J. Koehn, C. Shu, J. Sun, and R. J. Ho, "Long-acting three-drug combination anti-HIV nanoparticles enhance drug exposure in primate plasma and cells within lymph nodes and blood," (in eng), *AIDS,* vol. 28, no. 17, pp. 2625-7, Nov 2014.

[43] E. Gullberg *et al.*, "Expression of specific markers and particle transport in a new human intestinal M-cell model," (in eng), *Biochem Biophys Res Commun,* vol. 279, no. 3, pp. 808-13, Dec 2000.

[44] S. Cai, Q. Yang, T. R. Bagby, and M. L. Forrest, "Lymphatic drug delivery using engineered liposomes and solid lipid nanoparticles," (in eng), *Adv Drug Deliv Rev,* vol. 63, no. 10-11, pp. 901-8, Sep 2011.

[45] N. L. Trevaskis, L. M. Kaminskas, and C. J. Porter, "From sewer to saviour - targeting the lymphatic system to promote drug exposure and activity," (in eng), *Nat Rev Drug Discov,* vol. 14, no. 11, pp. 781-803, Nov 2015.

[46] A. Owen and S. Rannard, "Strengths, weaknesses, opportunities and challenges for long acting injectable therapies: Insights for applications in HIV therapy," (in English), *Advanced Drug Delivery Reviews,* Review vol. 103, pp. 144-156, Aug 2016.

[47] L. M. Tatham, A. C. Savage, A. B. Dwyer, M. Siccardi, S. P. Rannard, and A. Owen, "Towards a Maraviroc Long-Acting Injectable Nanoformulation," *Eur. J. Pharm. Biopharm,* Submitted 2018.

Figures

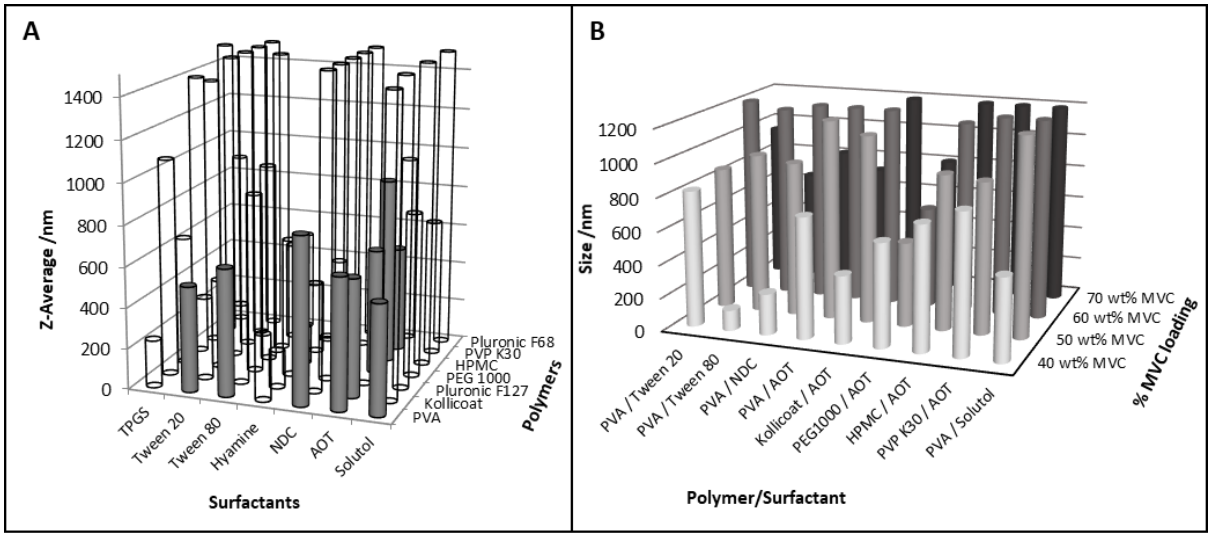

Figure 1: (A) 49 screen of 30 wt% Maraviroc SDNs, containing 30 wt% MVC, 55 wt% Polymer and 15 wt% Surfactant. 'Hits' highlighted in grey meet the following criteria: Size < 1000 nm, PDI < 0.4, Standard deviation < 15% and fully dispersible in water. (B) MVC SDNs formulations with increased MVC loadings, measured by DLS. Formulations were prepared as follows: 40 wt% MVC, 45 wt% Polymer and 15 wt% Surfactant; 50 wt% MVC, 50 wt% Polymer and 10 wt% Surfactant; 60 wt% MVC, 30 wt% Polymer and 10 wt% Surfactant; 70 wt% MVC, 20 wt% Polymer and 10 wt% Surfactant.

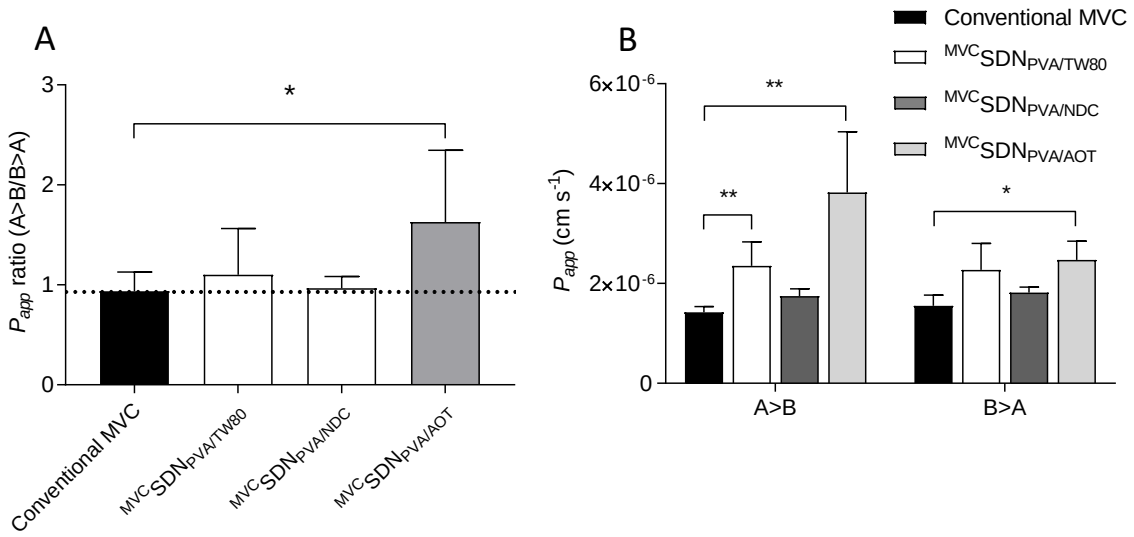

Figure 2. (A). Apparent oral absorption (P_{app} ratio) and (B) apparent permeability (P_{app} cm s^{-1}) of a conventional [^{3}H]-MVC preparation (<0.5% DMSO) and three [^{3}H]-MVC nanosuspensions across differentiated Caco-2 monolayers following 1 h incubation at 37^{o}C, 5% CO_2. *, P <0.05; **, P <0.01 (unpaired, two-tailed t-test) (n=4).

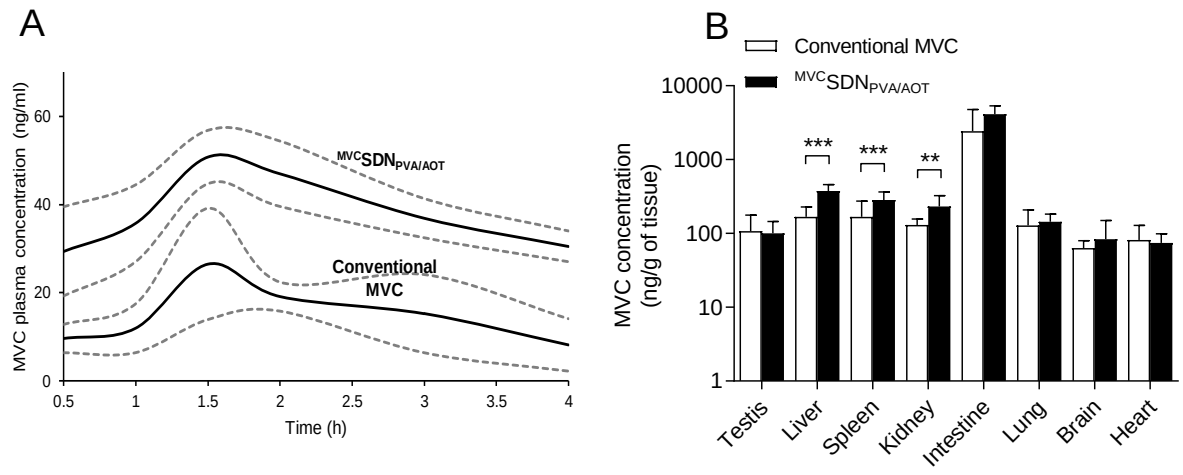

Figure 3. (A). MVC exposure in adult male Wistar rats following oral dosing of [^{3}H]-MVC 10 mg Kg^{-1} as a conventional preparation (<5% DMSO) or as a MVC nanodispersion, $^{MVC}SDN_{PVA/AOT}$. The fragmented lines give the standard deviations of the mean for four rats in each group. (B). Tissue distribution of [^{3}H]-MVC in adult male Wistar rats following oral dosing of [^{3}H]-MVC 10 mg Kg^{-1} as a conventional preparation (<5% DMSO) or as a MVC nanodispersion, $^{MVC}SDN_{PVA/AOT}$. Data are given as the mean ± standard deviation for four rats in each group. **, P <0.01; ***, P <0.001 (unpaired, two-tailed t-test).

Tables

Table 1. Z-average and PDI of candidates at 30 – 70 wt% loading.

MVC loading		30 wt%		40 wt%		50 wt%		60 wt%		70 wt%	
Polymer	**Surfactant**	**Z-Av /nm**	**PDI**	**Z-Av /nm**	**PDI**	**Z-Av /nm**	**PDI**	**Z-Av /nm**	**PDI**	**Z-Av /nm**	**PDI**
PVA	Tween 20	517	0.30	815	0.60	855	0.38	1247	0.31	950	0.34
PVA	Tween 80	623	0.29	122	0.41	957	0.48	1161	0.26	658	0.20
PVA	NDC	816	0.36	246	0.40	926	0.31	1750	0.31	823	0.17
PVA	AOT	643	0.35	724	0.36	1196	0.36	1205	0.26	728	0.30
Kollicoat	AOT	581	0.27	404	0.47	1124	0.56	1278	0.40	1550	0.71
PEG1000	AOT	612	0.25	620	0.55	507	0.46	608	0.37	815	0.58
HPMC	AOT	913	0.14	747	0.43	931	0.31	1150	0.45	1824	0.38
PVP K30	AOT	523	0.35	840	0.84	908	0.58	1951	0.46	3600	0.30
PVA	Solutol	538	0.34	494	0.39	1193	0.47	1392	0.30	1416	0.35

Table 2: Z-average diameter, polydispersity index and zeta potential of the three 70 wt% formulations

Formulation	Z-Average /nm	Polydispersity Index	Zeta Potential /mV
$^{MVC}SDN_{PVA/TW80}$	658	0.2	-12.8
$^{MVC}SDN_{PVA/NDC}$	823	0.17	-16.6
$^{MVC}SDN_{PVA/AOT}$	728	0.3	-25.3

Table 3: Pharmacokinetic parameters derived from Fig. 3 A.

Pharmacokinetic parameter	Conventional MVC	$^{MVC}SDN_{PVA/AOT}$	P-value (unpaired, two-tailed t-test)
C_{max} (ng ml^{-1})	26.52	50.74	P=0.0190
C_{min} (ng ml^{-1})	8.16	25.83	P=0.0309
AUC_{0-4} (ng.h ml^{-1})	58.71	145.33	P=0.0028
C_{avg} (ng ml^{-1})	15.17	38.38	P=0.0056
T_{max} (h)	1.5	1.5	-
C_{max}:C_{min} ratio	3.25	1.96	P=0.0828
C_{max}:C_{avg} ratio	1.75	1.32	P=0.0697
Half-life (t½) (h)	1.57	3.32	P=0.2153